

ISIR Journal of Multidisciplinary (ISIRJM)

ISSN: 3049-3080 (Online)

Frequency: Bimonthly

Published By ISIR Publisher

Journal Homepage Link- <https://isirpublisher.com/isirjm/>



Numerical Analysis of Velocity, Thermal, and Mass Slip Flow in MHD Micropolar Fluid Over a Stretching Sheet with Schmidt Number Effects

By

Mohammed Abdur Rahman

Department of Mathematics National University, Gazipur-1704, Bangladesh



Article History

Received: 05/06/2025

Accepted: 25/06/2025

Published: 29/06/2025

Vol – 1 Issue – 3

PP: -10-18

Abstract

This research examines the combined influences of the magnetic field and Schmidt number theoretically on the velocity, thermal, and mass slip flow of a micropolar fluid across a stretching sheet. An appropriate similarity transformation with the boundary conditions was used to alter the governing highly non-linear partial differential equations into non-linear ordinary differential equations. The gained non-linear ordinary differential equations are then solved numerically by the efficient method of shooting iteration coupled with an appropriate order of the Runge-Kutta integration scheme. The impacts of the diverse active dimensionless controlling parameters on the velocity, microrotation, temperature, and concentration profiles are examined, discussed, and presented through graphs. Furthermore, the values of the skin-friction, wall couple stress, Nusselt, and Sherwood numbers are calculated and offered using tables. Results showed that the local skin friction coefficient and the local Nusselt number decreased, whereas the local surface deposition flux increased with increasing thermal slip parameter. It is also depicted that with the increasing value of the velocity slip parameter, the local skin-friction coefficient and the local surface deposition flux decreased. The present solutions are compared with the previous related solutions in the literature in some limiting cases, showing an excellent agreement.

Keywords: Velocity, Thermal, and Mass Slips, Micropolar Fluid, MHD, Stretching Sheet, Schmidt Number

1. Introduction

Researchers have paid great attention to non-Newtonian fluids due to their widespread use in practical and real-world applications in numerous industrial processes. Various fluids, such as liquid crystals, crude oil, body fluids, polymers, exotic lubricants, paints, colloidal fluids, etc., are included in non-Newtonian fluids. Based on diverse fluid characteristics, non-Newtonian fluids have been formulated into different models, e.g., Casson fluid, Maxwell fluid, Jeffery fluid, and Micropolar fluids (Chen et al. [1]). During the last few decades, the micropolar fluid model has been the most popular model for non-Newtonian fluids. The theory of micro-polar fluids was first formulated by Eringen [2]. Micropolar fluid has a large range of use in different branches of science and engineering, like contaminated and clean engine lubricant fluids, complex biological structures, thrust-bearing technologies, cervical flows, radial diffusion paint rheology, colloids, and polymeric solutions (Singh et al. [3]). Many research workers ([4]-[11]) have reported their solutions on micropolar fluid flow for various physical

phenomena. Vanitha et al. [12] studied heat and mass transfer of micropolar liquid flow due to porous stretching/shrinking surface with ternary particles. Recently, a computation analysis and application with heat and mass transfer for micropolar fluid in ciliated microchannel were investigated by Imran et al. [13]. Very recently, Barman et al. [14] explored the stability of micropolar fluid flow in a vertical channel in the presence of thermal radiation and a transverse magnetic field.

The slip condition occurs at the solid-fluid interface where the standard no-slip condition does not hold. In the situation of velocity slip, fluid slips at the surface; that is, velocity is non-zero along the surface. Thermal slip refers to a discontinuity of temperature at the solid-fluid interface, mass slip refers to a discontinuity in the concentration of a species due to molecular diffusion at the boundary. Fluid behaviour, heat transfer, and mass transfer processes can be altered significantly caused by slip flow. It is known from the literature that slip boundary conditions are to be considered for low-pressure fluid flow or the system of flow with small



characteristic sizes for both stationary and moving boundaries when a particulate fluid like suspensions, emulsions, polymer solutions, and foams is used ([15]-[17], Wang [18]). The importance of slip velocity effects in different flow types was studied by researchers such as [19-23]. Mansour et al. [24] discussed analytically the MHD flow of a micropolar fluid due to heat and mass transfer through a porous medium bounded by an infinite vertical porous plate in a transverse magnetic field in a slip-flow regime. Recently, a two-dimensional, unsteady, forced flow of an incompressible, laminar micropolar nanofluid past a stretching sheet has been investigated numerically considering zero mass flux, velocity slip, and thermal slip boundary conditions by Rahman et al. [25]. Very recently, Singh et al. [3] focused on the combined impact of heat source/sink and chemical reaction on the slip flow of micropolar fluid through a permeable wedge in the existence of Hall and ion-slip currents.

The dimensionless parameter Schmidt number is frequently employed to analyze the mass transfer process, like diffusion and convection in a fluid flow system of heat and mass transfer. It relates the kinematic viscosity to the mass diffusivity of fluid. The amount to mix and spread and the thickness of the concentration of the boundary layer of micropolar fluids are determined by the Schmidt number. A high Schmidt number results in slower mixing and a low Schmidt number leads to faster diffusion. Numerous applications due to the effect of the Schmidt number are noted for mass transfer and fluid flow control in biomedical flows, microfluidics, and chemical processes. Researchers have gained valuable insights into how mass is transported within a medium by studying the Schmidt number ([26], [27], [28]). Recently, Srilatha et al. [29] found that concentration falls with a fall of Schmidt number in the study of the influence of MHD micropolar fluid flow over permeable stretching sheets with slip phenomena. Very recently, the analysis of hydromagnetic micropolar nanofluid over an inclined stretching sheet performed by Walegign [30] showed that for a value of the Schmidt number, the mass transfer grows.

Mass slip with zero-pressure gradient occurs when fluids move very slowly in small spaces, like in tiny lab devices, fine air or gas filters, or medical tools that handle fluids carefully. In these cases, the pressure remains almost the same. But in the case of a clear pressure difference, mass slip with a pressure gradient happens. This is common in oil recovery, where gas is used to push out oil, or in air cleaners and high-quality filters, to use pressure changes to move air and clean it. From the literature discussed above, we observed that mass slip with pressure gradient condition, which plays a significant role in fluid flow, has not been considered in any previous research. The innovation of the present investigation is to study the combined effects of transverse magnetic field, Prandtl number, and Schmidt number on heat and mass transfer in a convective micropolar fluid flow over a stretched sheet under slip flow (velocity, thermal, and mass) conditions. Numerical solutions of the governing equations of the flow model have been found using the Nachtsheim-Swigert

iteration technique [31] along with the Runge-Kutta method of order six. Parameters on flow characteristics are represented by graphs drawn with the help of the plotting software Tecplot 10, and they are studied and discussed from a physical point of view. The results of our problem, compared with the results of a previously published paper, showed a significant level of consistency. To our knowledge, the considered flow model has not been examined with the process said above so far in the scientific literature available. Industrial applications such as cleaning, heat exchanging, polishing, and manufacturing processes could gain benefits from this type of research.

2. Problem formulation and description

We consider an incompressible, laminar, electrically conducting, viscous micropolar fluid flow of heat and mass transfer over a flat stretching sheet in the presence of velocity, thermal, and mass slip. It is also assumed that the constant temperature of the surface of the sheet is T_w and that of the surrounding fluid is T_∞ where $T_w > T_\infty$. A strong transverse magnetic field $B(x, t)$ of strength B_0 is applied perpendicular to both the flow direction and the sheet surface. The Schmidt number impact is also incorporated into the problem. The x and y axes are taken along the stretching sheet and normal to it, respectively. The velocity of the stretching sheet is assumed to be linear, while the upstream velocity is zero. The flow domain under consideration is confined to the region $y > 0$. The flow model and geometry of the current regular viscous problem are presented in Figure 1.

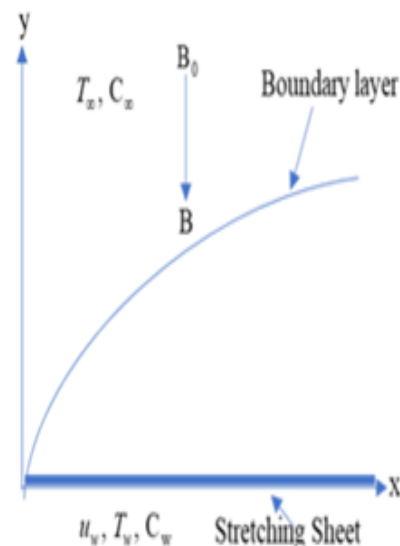


Figure 1: Laminar, electrically conducting fluid flow

Under these assumptions and boundary layer approximations, the governing equations and the corresponding boundary conditions are taken as follows (Rahman et al. [25] and Abbas et al. [32]):

$$\frac{\partial u}{\partial x} + \frac{\partial v}{\partial y} = 0, \tag{1}$$

$$\frac{\partial u}{\partial t} + u \frac{\partial u}{\partial x} + v \frac{\partial u}{\partial y} = K_1 \left(\frac{\partial u_e}{\partial t} + u_e \frac{\partial u_e}{\partial x} \right) + \left(\frac{\mu + \eta_v}{\rho} \right) \frac{\partial^2 u}{\partial y^2} + \frac{\eta_v}{\rho} \frac{\partial N}{\partial y} - \frac{\sigma_0 B^2(x,t)}{\rho} (u - u_e), \tag{2}$$

$$\frac{\partial N}{\partial t} + u \frac{\partial N}{\partial x} + v \frac{\partial N}{\partial y} = \frac{\sigma}{\rho j} \frac{\partial^2 N}{\partial y^2} - \frac{\eta_v}{\rho j} \left(2N + \frac{\partial u}{\partial y} \right), \tag{3}$$

$$\frac{\partial T}{\partial t} + u \frac{\partial T}{\partial x} + v \frac{\partial T}{\partial y} = \frac{k}{\rho c_p} \frac{\partial^2 T}{\partial y^2}, \tag{4}$$

$$\frac{\partial C}{\partial t} + u \frac{\partial C}{\partial x} + v \frac{\partial C}{\partial y} = D \frac{\partial^2 C}{\partial y^2}, \tag{5}$$

With conditions:

$$\left. \begin{aligned} y \rightarrow 0: u &= \delta_0 u_w(x,t) + P_1(x,t) v \left(\frac{\partial u}{\partial y} \right), v=0, N = -n \frac{\partial u}{\partial y}, \\ T &= T_w(x,t) + E_1(x,t) \left(\frac{\partial T}{\partial y} \right), C = C_w(x,t) + F_1(x,t) \left(\frac{\partial C}{\partial y} \right) \\ y \rightarrow \infty: u &= K_1 u_e(x,t), N \rightarrow 0, T \rightarrow T_\infty, C \rightarrow C_\infty \end{aligned} \right\} \tag{6}$$

Here, u (velocity components along x -axis), v (velocity components along y -axis), t (time), K_1 (pressure gradient), μ (coefficient of dynamic viscosity), η_v (vortex viscosity), ρ (micropolar fluid density), σ_0 (electrical conductivity), N (microrotation component normal to xy -plane), σ (spin-gradient viscosity), j (micro-inertia density), T (fluid temperature), c_p (specific heat at constant pressure), k (thermal conductivity), C (fluid concentration), D (molecular diffusivity), δ_0 (stretching constant), $B(x,t) = \frac{B_0}{\sqrt{1-\beta_0 t}}$ (transverse magnetic field), $P_1(x,t) = (P_1)_0 \sqrt{\nu(1-\beta_0 t)^3/a}$ (velocity slip factor), V (kinematic viscosity), $E_1(x,t) = (E_1)_0 \sqrt{\nu(1-\beta_0 t)^3/a}$ (thermal slip factor), $F_1(x,t) = (F_1)_0 \sqrt{\nu(1-\beta_0 t)^3/a}$ (mass slip factor), $(P_1)_0$, $(E_1)_0$ and $(F_1)_0$ (constant velocity, thermal, and mass slip factor), $u_w(x,t) = u_e = (ax)/(1-\beta_0 t)$ (surface fluid velocity varying with the coordinates x and t), $T_w(x,t) = T_\infty + (bx)/(1-\beta_0 t)^2$ (surface fluid temperature varying with the coordinates x and t),

$C_w(x,t) = C_\infty + (cx)/(1-\beta_0 t)^2$ (surface fluid concentration varying with the coordinates x and t), C_∞ (fluid concentration outside the boundary layer), a and β_0 (positive constant having dimension per time), b and c (constants with dimensions of temperature and concentration), n (particle concentration difference), $n=0$ (no-spin condition) (Peddieson [33]), $n=0.5$ (weak concentration) (Ahmadi [34]), $n=1$ (turbulent flow) (Jena and Mathur [4]).

To simplify the field equations (1)-(6) we introduce the dimensionless parameters:

$$\left. \begin{aligned} \eta(y,t) &= \sqrt{\frac{a}{\nu(1-\beta_0 t)}} y, \psi(x,y,t) = \sqrt{\frac{\nu a}{(1-\beta_0 t)}} x f(\eta), N(x,y,t) = \sqrt{\frac{a^3}{\nu(1-\beta_0 t)}} x h(\eta), \\ T &= T_\infty + \frac{b}{(1-\beta_0 t)^2} x \theta(\eta), C = C_\infty + \frac{c}{(1-\beta_0 t)^2} x \varphi(\eta), \theta(\eta) = \frac{T-T_w}{T_\infty-T_w}, \varphi(\eta) = \frac{C-C_\infty}{C_w-C_\infty} \end{aligned} \right\} \tag{7}$$

where $\eta(y,t)$ (independent similarity variable), $\psi(x,y,t)$ (stream function), $f(\eta)$ (dimensionless linear velocity), $h(\eta)$ (dimensionless microrotation), $\theta(\eta)$ (dimensionless temperature), and $\varphi(\eta)$ (dimensionless concentration). The problem becomes steady with $\beta_0 = 0$.

The obtained dimensionless system is as follows:

$$(1+\Delta)f''' + ff'' - (f')^2 - \frac{U}{2}(2f' + \eta f''') + \Delta h' + K_1(1+U) - 2M_n(f' - 1) = 0, \quad (8)$$

$$\xi h'' + fh' - f'h - \frac{U}{2}(3h + \eta h') - \Delta V(2h + f''') = 0, \quad (9)$$

$$\theta'' + \text{Pr}(f\theta' - f'\theta) - \frac{\text{Pr}U}{2}(4\theta + \eta\theta') = 0, \quad (10)$$

$$\phi'' - \frac{USc}{2}(4\phi + \eta\phi') - Sc(f'\phi - f\phi') = 0, \quad (11)$$

with conditions:

$$\left. \begin{aligned} \eta \rightarrow 0: f(\eta) = 0, f'(\eta) = \lambda_0 + \delta_v f''(\eta), h(\eta) = -\eta f''(\eta), \\ \theta(\eta) = 1 + \delta, \theta'(\eta), \phi(\eta) = 1 + \delta_c \phi'(\eta), \\ \eta \rightarrow \infty: f'(\eta) = K_1, h(\eta) = 0, \theta(\eta) = 0, \phi(\eta) = 0 \end{aligned} \right\} \quad (12)$$

where, $\Delta = \frac{\eta_v}{\mu}$ (vortex viscosity parameter), $U = \frac{\beta_0}{a}$

(unsteadiness parameter), $M_n = \frac{\sigma_0 B_0^2}{\rho \beta_0}$ (magnetic field

parameter), $\xi = \frac{\sigma}{\mu j}$ (spin-gradient viscosity parameter),

$V = \frac{\nu(1 - \beta_0 t)}{ja}$ (micro-inertia density parameter),

$\text{Pr} = \frac{\nu \rho c_p}{k}$ (Prandtl number), $Sc = \frac{\nu}{D}$ (Schmidt number).

The equations of physical quantities for engineering interests are derived as follows:

$$\text{Local skin-friction coefficient: } Cf_x = \frac{2(1+\Delta)f''(0)}{\sqrt{\text{Re}_x}} \quad (13)$$

$$\text{Local wall couple stress coefficient: } M_x = \frac{(2+\Delta)\xi}{1+\Delta} h'(0) \quad (14)$$

$$\text{Local Nusselt number: } Nu_x = -\sqrt{\text{Re}_x} \theta'(0) \quad (15)$$

$$\text{Local Stanton number: } St_x = -\frac{axC_\infty}{Sc\sqrt{\text{Re}_x}} \phi'(0) \quad (16)$$

3. Method and study comparison

The set of highly non-linear and coupled differential equations with boundary conditions expressed by (8)-(12) was numerically solved by applying the Nachtsheim-Swigert shooting iteration with the sixth-order Runge-Kutta method. Initial guess values were assumed for the unspecified boundary conditions. The Runge-Kutta method integrated the equations step by step from the sheet surface to the fluid domain, and the Nachtsheim-Swigert technique adjusted the guessed values to satisfy the boundary conditions far away from the surface. This process was repeated until the difference between two consecutive steps became less than

10^{-5} , ensuring the convergence. The numerical technique described above was implemented using a FORTRAN program, which was executed on a computer to obtain the desired numerical results.

The present numerical results of the dimensionless shear stress $f''(0)$ for various values of the velocity slip parameter δ_v with $\Delta = \lambda_0 = 3.0$, $\xi = 2.0$, $n = 0.5$, $\text{Pr} = 7.0$, $M_n = \delta_T = V = 0.1$, $U = 1.0$, $K_1 = \delta_c = 0.0$, $Sc = 0.63$ show a good agreement with those of Rahman et. Al. [25] as shown in **Table 1** below.

Table 1: Validation of the present results with the established results

δ_v	$f''(0)$	
	Rahman et. al. [25]	Present results
0.1	0.0318	0.0315
0.5	0.0316	0.0313
1.0	0.0313	0.0310
1.5	0.0309	0.0306

3. Results and discussion

To find out the numerical solutions of the present problem of velocity, thermal, and mass slip flow in magnetohydrodynamic micropolar fluid over a stretching sheet with Schmidt number, we fixed the parameter values such as $\Delta = \lambda_0 = 3.0$, $\xi = 2.0$, $n = 0.5$, $\text{Pr} = 7.0$, $M_n = \delta_v = \delta_T = \delta_c = V = 0.1$, $U = 1.0$, $K_1 = 0.0$ unless otherwise stated, and $Sc = 0.63$ throughout the calculation in the program code, except for the parameter whose effect was investigated. The impact of different values of a definite parameter is found in the velocity, microrotation, temperature, and concentration, which consist of the numerical values obtained from the solution.

Effects of distinct values of Mn , λ_0 , Δ , and U on velocity profiles are displayed in Figures 2(a)-(d), respectively. It is seen from Figure 2(a) that the velocity decreases with increasing magnetic field parameter Mn . A stronger magnetic field (higher Mn) slows down the fluid due to the opposing Lorentz force and thus reduces the hydrodynamic boundary layer thickness. Figure 2(b) shows that the velocity increases with higher stretching sheet parameter λ_0 . As λ_0 rises, the sheet stretches more rapidly, enhancing the fluid velocity near the surface. As a result, the boundary layer becomes thicker. Velocity increases significantly with an increase in the vortex viscosity parameter Δ as observed in Figure 2(c). Increasing the value of the unsteadiness

parameter U enhances the fluid velocity close to the surface, whereas it decreases rapidly far away from the surface, as depicted in Figure 2(d). This indicates a thinner boundary layer with increasing U which is typical in unsteady flow scenarios.

Figures 3(a)-(e) describe the influence of the parameters V , n , ξ , U , and Δ on microrotation profiles. Overall, it is noticed that the microrotation profiles increase with higher micro-inertia density V , microrotation parameter n , and vortex viscosity parameter Δ indicating stronger

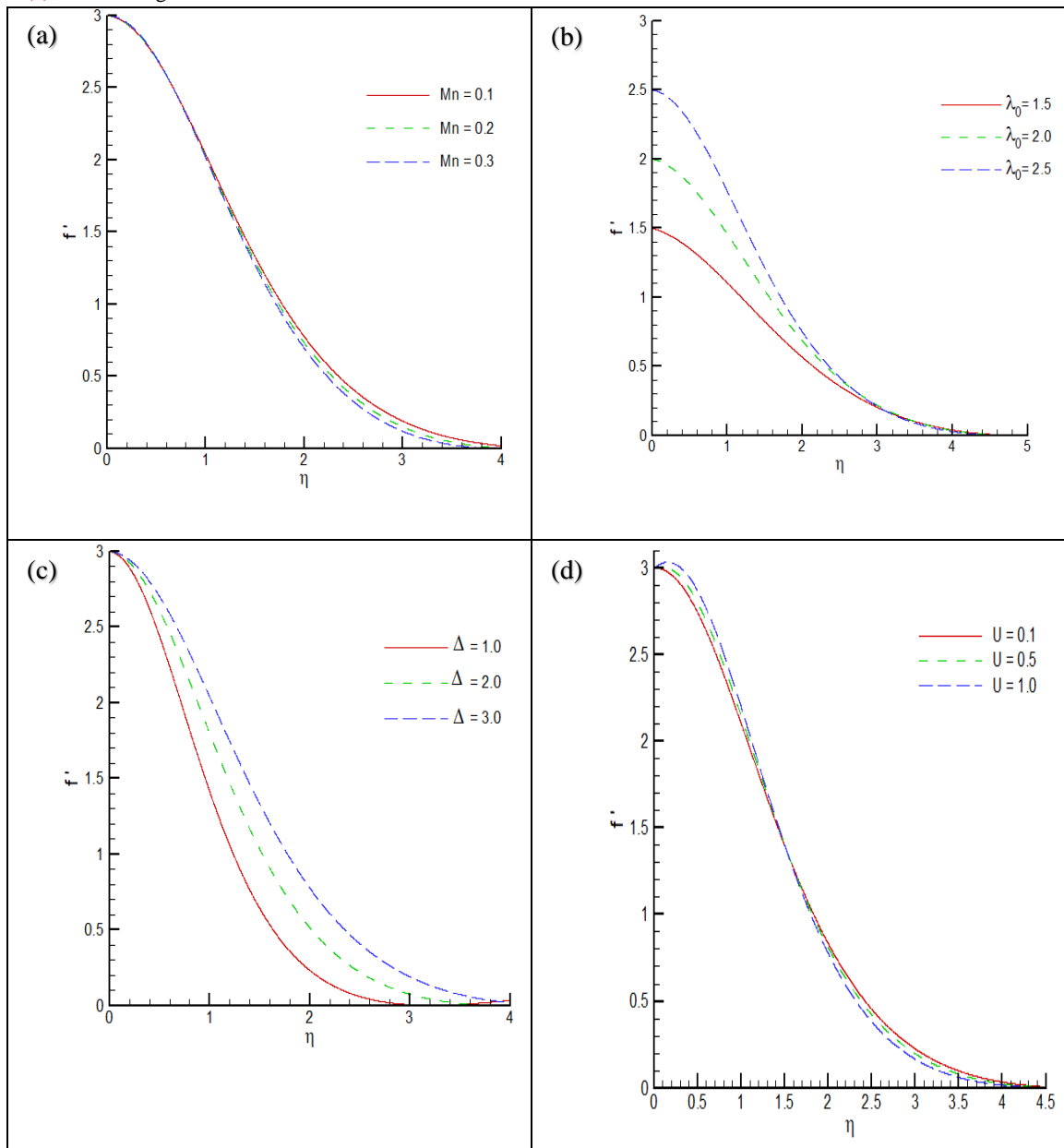


Figure 2: Effect of distinct values of (a) Mn (b) λ_0 (c) Δ , and (d) U velocity.

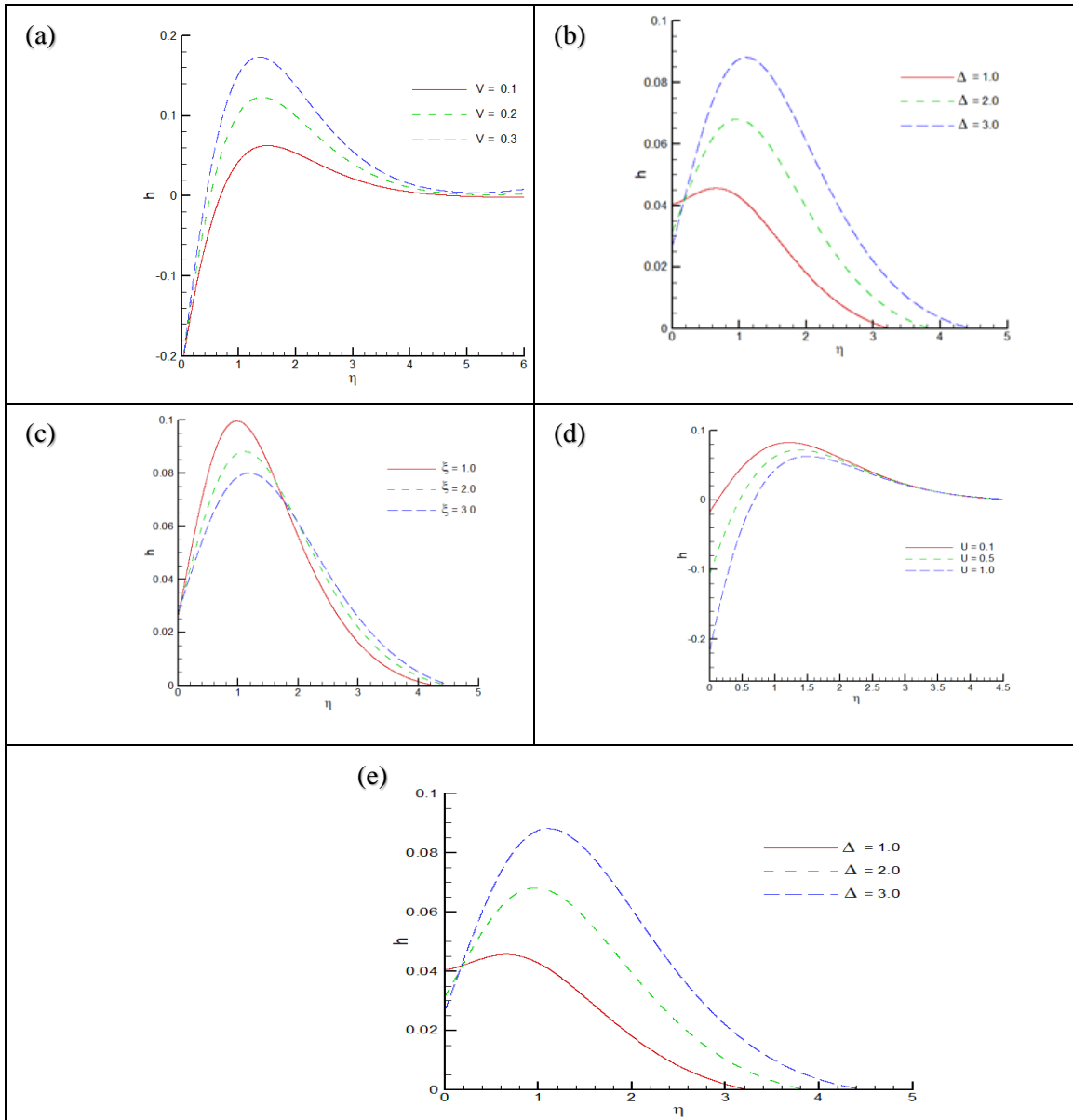


Figure 3: Effect of distinct values of (a) V (b) n (c) ξ (d) U , and (e) Δ on microrotation.

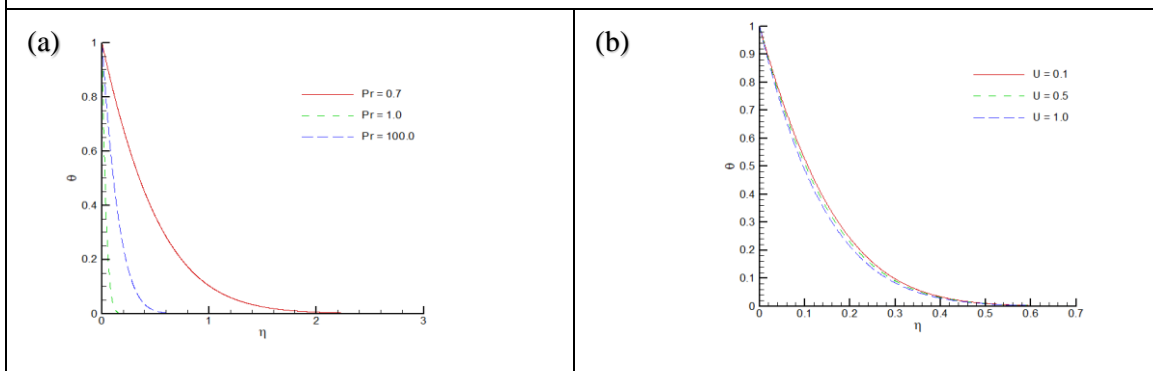


Figure 4: Effect of distinct values of (a) Pr , and (b) U on temperature.

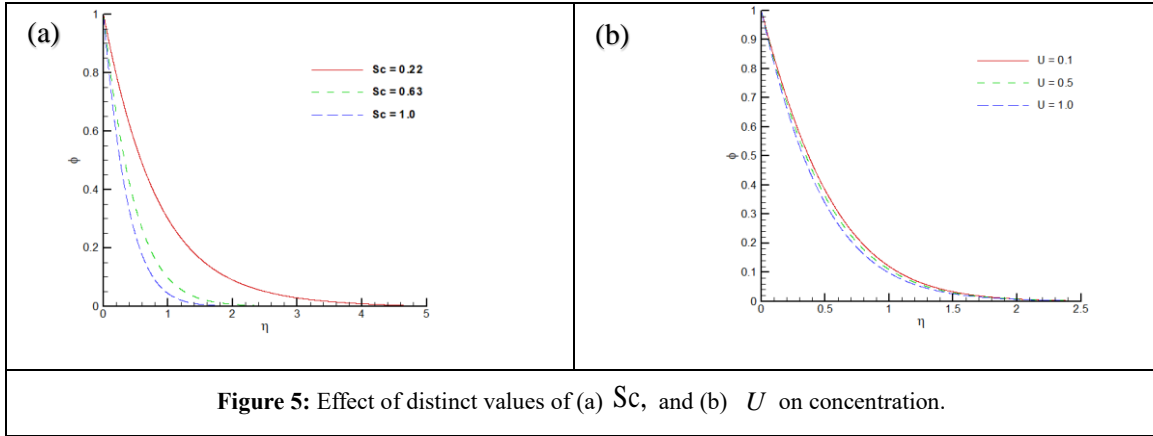


Figure 5: Effect of distinct values of (a) Sc , and (b) U on concentration.

Table 2: Values of local skin-friction coefficient, local wall couple stress coefficient, local Nusselt number, and local Stanton number for variation in δ_T with zero pressure gradient.

δ_T	$f''(0)$	$h'(0)$	$-\theta'(0)$	$-\phi'(0)$
1.0	0.03340451	0.14651597	-5.83065221	-1.70871052
1.5	0.03340451	0.14651597	-5.83065017	-1.70871052
2.0	0.03340451	0.14651597	-5.83064623	-1.70871052
2.5	0.03340451	0.14651597	-5.83064051	-1.70871052

Table 3: Values of local skin-friction coefficient, local wall couple stress coefficient, local Nusselt number, and local Stanton number for variation in U with zero pressure gradient.

U	$f''(0)$	$h'(0)$	$-\theta'(0)$	$-\phi'(0)$
0.1	0.03340451	0.14651597	-5.83065074	-1.70871052
0.5	0.21160587	0.28155785	-6.22490577	-1.83823466
1.0	0.43276487	0.47059001	-6.68966191	-1.98861779

Table 4: Values of local skin-friction coefficient, local wall couple stress coefficient, local Nusselt number, and local Stanton number for variation in V with zero pressure gradient.

V	$f''(0)$	$h'(0)$	$-\theta'(0)$	$-\phi'(0)$
0.1	0.43276487	0.47059001	-6.68966191	-1.98861779
0.2	0.43703504	0.55777367	-6.69019189	-1.98972958
0.3	0.43972903	0.62816036	-6.69057412	-1.99058265

Table 5: Values of local skin-friction coefficient, local wall couple stress coefficient, local Nusselt number, and local Stanton number for variation in Sc with zero pressure gradient.

Sc	$f''(0)$	$h'(0)$	$-\theta'(0)$	$-\phi'(0)$
0.22	0.42967123	0.46812030	-6.68946779	-1.14517876
0.63	0.43703504	0.55777367	-6.68965937	-1.98972958
1.0	0.43876487	0.47059001	-6.69019189	-2.51719216

Table 6: Values of local skin-friction coefficient, local wall couple stress coefficient, local Nusselt number, and local Stanton number for variation in δ_C with zero pressure gradient.

δ_c	$f''(0)$	$h'(0)$	$-\theta'(0)$	$-\phi'(0)$
1.0	0.43276487	0.47059001	-6.68965616	-1.98862705
1.5	0.43276487	0.47059001	-6.68965090	-1.98863658
2.0	0.43276487	0.47059001	-6.68964598	-1.98864614

Table 7: Values of local skin-friction coefficient, local wall couple stress coefficient, local Nusselt number, and local Stanton number for variation in pressure gradient K_1 .

K_1	$f''(0)$	$h'(0)$	$-\theta'(0)$	$-\phi'(0)$
0.0	0.43276487	0.47059001	-6.68966191	-1.98861779
0.01	0.41444900	0.45523007	-6.68854357	-1.98750295
0.02	0.39658751	0.44026363	-6.68745272	-1.98641477

rotational effects. In contrast, increasing the spin-gradient viscosity parameter ξ , and the unsteadiness parameter U reduce microrotation profiles, showing a damping effect. Thus, V , n , and Δ promote microrotation, making it stronger, while ξ , and U suppress to weaken the microrotation. Each parameter affects the magnitude and distribution of rotational motion in distinct ways.

Figures 4(a)-(b) exhibit the effects of the Prandtl number Pr , and the unsteadiness parameter U , respectively, on the temperature profiles. From the figures, a decrease in the temperature profiles is observed with higher values of both Pr , and U , with the increase of the independent similarity variable η . This is expected because increasing values of these parameters enhance thermal diffusion, which causes lower temperatures. This results in the boundary layer becoming thinner. However, the contribution of the parameter Pr on the temperature distribution is significantly more pronounced than that of the parameter U . This effect is useful for controlling heat in microfluidics, medical flows, lubrication systems, cooling systems, and spacecraft under slip conditions.

Figures 5(a) and (b), respectively, illustrate the variation of the Schmidt number Sc and unsteadiness parameter U on the concentration profiles. Figure 5(a) shows the concentration profile against the independent similarity variable η for different values of Sc . It is observed that the concentration decreases more quickly with increasing Sc . This is expected because a higher Schmidt indicates lower mass diffusivity, resulting in a thinner concentration boundary layer. It is observed from Figure 5(b) that the concentration decreases slowly as U increases. This occurs because higher values of U reduce solute diffusion from the surface, resulting in a thinner concentration boundary layer.

Under zero pressure gradient, we observe varied behaviors based on different parameters. In Tables 2 and 6, the local skin-friction coefficient and local wall couple stress

coefficient remain unchanged throughout, while the local Nusselt number increases, showing improved heat transfer with thermal and mass slip, respectively. In Tables 3-5, the local Nusselt and Stanton numbers consistently decrease with increases in unsteadiness, micro-inertia density, and Schmidt number, indicating reduced thermal performance. Additionally, local skin-friction coefficient increases in all three cases, while local wall couple stress shows mixed behavior, rising in Tables 3-4, first increasing and then decreasing in Table 5.

Both the local skin-friction and the local wall couple stress coefficients decrease, while the local Nusselt and Stanton numbers increase with the increase in the values of pressure gradient, as noted in Table 7. This reflects enhanced heat and momentum transport under pressure-driven flow, contrasting with the trends observed under zero pressure gradient conditions.

4. Conclusions

The study numerically investigates the effects of various physical parameters on velocity, microrotation, temperature, and concentration in an MHD micropolar fluid with slip conditions over a stretching sheet. Practitioners can take help from the results to make decisions in practical flow situations and industrial work. The key findings are as follows:

1. The velocity decreases with a stronger magnetic field while it increases with vortex viscosity, higher stretching rate, and unsteadiness near the surface.
2. With micro-inertia density, microrotation parameter, and vortex viscosity, microrotation increases whereas it decreases with spin-gradient viscosity and unsteadiness.
3. Temperature and concentration profiles reduce with increasing Prandtl number, Schmidt number, and unsteadiness, resulting in thinner thermal and concentration boundary layers.
4. Under zero pressure gradient, thermal and mass slip enhance heat transfer (higher Nusselt number), while unsteadiness, Schmidt number, and micro-inertia density reduce thermal performance.

- Heat and mass transfer improve- local Nusselt and Stanton numbers increase, and local skin-friction and wall couple stress decrease, indicating more efficient flow, in the presence of a pressure gradient.

References

- Chen, J., Liang, C. and Lee, J. D., Theory and Simulation of Micropolar Fluid Dynamics. *Journal of Nanoengineering and Nanosystems*, 2011, **224**, 31-39.
- Eringen, A. C., Theory of micropolar fluid. *J. Math. Mech.*, 16, 1-18.
- Singha, K., Pandeyb, A. K., and Kumar, M., Slip flow of micropolar fluid through a permeable wedge due to the effects of chemical reaction and heat source/sink with Hall and ionslip currents: an analytic approach. *Propulsion and Power Research*, 2020, 9(3), 289-303.
- Ahmadi, G., Self-similar solution of incompressible micropolar boundary layer flow over a semi-infinite plate. *Int. Jour. Engg. Sci.*, 1976, 14, 639 -646.
- Qukaszewicz, G., *Micropolar Fluids Theory and Application*, Birkhäuser, Basel, 1999.
- Ishak, A., Nazar, R., and Pop, I., Flow of a micropolar fluid on a continuous moving surface. *Archi. Mechs.*, 2006, 58, 529-541.
- Rahman, M. M., and Sattar, M. A. Transient convective flow of micropolar fluid past a continuously moving vertical porous plate in the presence of radiation. *Int. Jour. Appl. Mech. Eng.*, 2007, 12, 497-513.
- Ishak, A., Nazar, R., and Pop, I., Magnetohydrodynamic flow of a micropolar fluid towards a stagnation point on a vertical surface. *Comp. Math. Appl.*, 2008, **56**, 3188-3194.
- Ashraf, M., and Ashraf, M. M., MHD stagnation point flow of a micropolar fluid towards a heated surface. *Appl. Math. Mech. Eng. Ed*, 2011, 32, 45-54.
- El-Aziz, M. A., Corrigendum: Viscous Dissipation Effect on Mixed Convection Flow of a Micropolar Fluid Over an Exponentially Stretching Sheet. *Can. J. Phys.*, 2009, 87, 359-368. <https://doi.org/10.1139/p11-079>
- Bhattacharyya, K., Mukhopadhyay, S., Layek, G., and Pop, I., Effects of thermal radiation on micropolar fluid flow and heat transfer over a porous shrinking sheet. *Int. J. Heat Mass Trans.*, 2012, 55, 2945-2952.
- Vanitha, G. P., Mahabaleswar, U. S., Hatami, M., and Yang, X., Heat and mass transfer of micropolar liquid flow due to porous stretching/shrinking surface with ternary nanoparticles. *Scientific Reports*, 2023, 13, 3011. <https://doi.org/10.1038/s41598-023-29469-0>
- Imran, A., Alzubadi, H., and Ali, M. R., A computation analysis with heat and mass transfer for micropolar nanofluid in ciliated microchannel: With application in the ductus fferentes. *Heliyon*, 2024, 10 (19), e39018. <https://doi.org/10.1016/j.heliyon.2024.e39018>
- Barman, P, and Srinivasacharya, D, Influence of radiation on the stability of MHD micropolar fluid in a vertical channel. *European Journal of Mechanics - B/Fluids*, 2025, 109, 80-91. <https://doi.org/10.1016/j.euromechflu.2024.09.003>
- Shikhmurzaev, Y. D., The moving contact line on a smooth solid surface. *Int. J. Multiph Flow*, 1993, 19, 589-610.
- Choi, C. H., Westin, J. A., and Breuer, K. S., To slip or not to slip water flows in hydrophilic and hydrophobic microchannels. In *Proceedings of IMECE*, New Orleans, LA, Paper No. 2002-33707, 2002.
- Martin, M. J., and Boyd, I. D., Blasius boundary layer solution with slip flow conditions, Presented at the 22nd Rarefied Gas Dynamics Symposium, Sydney, Australia, 2000.
- Wang, C. Y., Flow Due to Stretching Boundary with Partial Slip-An Exact Solution of the Navier Stokes Equation. *Chemical Engineering Science*, 2002, 57, 3745-3747. [https://doi.org/10.1016/S0009-2509\(02\)00267-1](https://doi.org/10.1016/S0009-2509(02)00267-1)
- Mahmoud, M. A. A., and Waheed, S. E., MHD flow and heat transfer of a micropolar fluid over a stretching surface with heat generation (absorption) and slip velocity, *J. Egyptian Math. Soc.*, 2012, **20**, 20-27.
- Das, K., Slip effects on MHD mixed convection stagnation point flow of a micro-polar fluid towards a shrinking vertical sheet, *Comput. Math. Appl.*, 2012, 63, 255-267.
- Rosca, N. C., and Pop, I., Boundary layer flow past a permeable shrinking sheet in a micropolar fluid with a second order slip flow model, *European J. Mech. B/Fluids*, 2014, 48, 115-122.
- Das, K., Jana, S., and Kundu, P. K., Thermophoretic MHD slip flow over a permeable surface with variable fluid properties, *Alexandria Eng. J.*, 2015, 54 35-44.
- Singh, P. P., Pandey, A. K. and Kumar, M., Forced convection in MHD slip flow of alumina-water nanofluid over a flat plate, *J. Enhanc. Heat Transf.*, 2016, 23 (6), 487-497.
- Mansour, A. M., Mohamed, R. A., Abd-Elaziz, M. M., and Ahmed, S. E., Fluctuating thermal and mass diffusion on unsteady MHD convection of a micropolar fluid through a porous medium past a vertical plate slip-flow regime. *Int. J. of Appl. Math and Mech.* 2007, 3 (3), 99-117.
- Rahman, M. A., Uddin, M. J., and Alim, M. A., Unsteady forced convection slip flow of micropolar nanofluid over vertical stretching sheet with magnetic field. *Journal of Engineering Science*, 2017, 08(1), 109-118.

26. Tominaga, Y., and Stathopoulos, T., Turbulent Schmidt numbers for CFD analysis with various types of flowfield. *Atmos, 2007, Environ.*, 41, 8091-8099, 10.1016/j.atmosenv.2007.06.054
27. Koutsou, C. P., Yiantsios, S. G., and Karabelas, A. J., A numerical and experimental study of mass transfer in spacer-filled channels: effects of spacer geometrical characteristics and Schmidt number. *J. Memb. Sci.*, 2009, 326, 234-251, 10.1016/j.memsci.2008.10.007
28. Srinivasan, M., and Ramasamy, P., Computational modeling on the influence of the schmidt number on second phase impurities SiC, Si₂N₂O and Si₃N₄ in grown mc-silicon for PV applications. *Silicon*, 2018, 10, 077-1085, 10.1007/s12633-017-9574-5
29. Srilatha, P., Hassan, A. M., Goud, B. S., and Kumar, E. R., Mathematical study of MHD micropolar fluid flow with radiation and dissipative impacts over a permeable stretching sheet: slip effects phenomena. *Frontiers in Heat and Mass Transfer*, 2023, 21, 539-562. <https://doi.org/10.32604/fhmt.2023.043023>
30. Walegign, T., and Seid, E., Mathematical model analysis for hydromagnetic flow of micropolar nanofluid with heat and mass transfer over inclined surface. *International Journal of Thermofluids*, 2024, 21, 100541. <https://doi.org/10.1016/j.ijft.2023.100541>
31. Nachtsheim, P. R., and Swigert, P., Satisfaction of the asymptotic boundary conditions in numerical solution of the systems of non-linear equations of boundary layer type, Ph.D. Thesis, NASA TN D-3004, Washington DC, 1965.
32. Abbas T., Khan S. U., Saeed M., Khan M. I., Ismail E. A. A., Awwad F. A. and Abdullaeva B. S., 2024. Thermal stability and slip effects in micropolar nanofluid flow over a shrinking surface: A numerical study via Keller box scheme with block-elimination method, *AIP Adv.* 14(8), 085102.
33. Peddieson, J. (1972) An Application of the Micropolar Model to the Calculation of a Turbulent Shear Flow. *International Journal of Engineering Science*, 10, 23-32.
34. Jena, S.K. and Mathur, M.N. (1981) Similarity Solutions for Laminar Free Convection Flow of a Thermomicropolar Fluid past a Non-Isothermal Flat Plate. *International Journal of Engineering Science*, 19, 1431-1439.